Dielectric Relaxation and Thermally Stimulated Discharge Currents in Liquid-Crystalline Side-Chain Polymethacrylates with Phenylbenzoate Mesogens Having Tail Groups of Different Le...

ARTICLE *in* MACROMOLECULES · JULY 2003

Impact Factor: 5.8 · DOI: 10.1021/ma020832c

5 AUTHORS, INCLUDING:

E.B. Barmatov
Schlumberger Limited
114 PUBLICATIONS **580** CITATIONS
SEE PROFILE

Ricardo Díaz-Calleja
Universitat Politècnica de València
223 PUBLICATIONS **1,720** CITATIONS
SEE PROFILE

Dielectric Relaxation and Thermally Stimulated Discharge Currents in Liquid-Crystalline Side-Chain Polymethacrylates with Phenylbenzoate Mesogens Having Tail Groups of Different Length

Natalia Nikonorova* and Tamara Borisova

Institute of Macromolecular Compounds of the Russian Academy of Sciences, Bolshoy pr. 31, 199004 St. Petersburg, Russia

Evgueni Barmatov

Chemistry Department, Moscow State University, 119899 Moscow, Russia

Polycarpos Pissis

Department of Physics, National Technical University of Athens, Zografou Campus, 15780 Athens, Greece

Ricardo Diaz-Calleja

Department of Applied Thermodynamics, Polytechnic University of Valencia, 4606 Valencia, Spain

Received May 28, 2002; Revised Manuscript Received January 27, 2003

ABSTRACT: Molecular dynamics of six side-chain liquid-crystalline polymethacrylates with phenylbenzoate mesogenic groups having tail groups of different lengths was investigated by dielectric spectroscopy (DS) and by thermally stimulated discharge current (TSDC) methods. In the temperature range from room temperature to 160 °C, three processes of relaxation of dipole polarization, the β_1, α, and δ processes, were revealed. These correspond, from low to high temperatures, to the mobility of ester groups adjoining the backbone, to the segmental motion, and to the mesogenic group orientation about its short axis. For a quantitative analysis, dielectric spectra were described by a superposition of one or of two Havriliak−Negami functions and of a conductivity term. It was shown that the molecular mobility of the observed relaxation processes does not depend on the mesogen tail length. The comparison of the DS and TSDC data with each other gives good agreement between the temperature position of dielectric loss peaks at the equivalent frequency of TSDC measurements and the temperature position of depolarization current maximum. By using thermal windowing techniques, the activation parameters for the observed processes were determined.

1. Introduction

The classical method of dielectric spectroscopy (DS) makes it possible to investigate processes of relaxation of dipole polarization in polymers and, in particular, in side-chain liquid-crystalline polymers (SCLCPs), which are not only of scientific but also of practical interest. The decoding of a dielectric spectrum allows us to identify the observed relaxation processes and to connect them with the mobility of certain kinetic units bearing a polar group. The possibility for decoding of dielectric spectra is based on the systematic, consecutive change in one element of the chemical structure of the macromolecule and on the comparison with each other of the dielectric behavior of systems with similar chemical structures.[1−3]

The method of thermally stimulated depolarization currents (TSDC) is also successfully used in the research of dipole polarization mechanisms in polymers. The results obtained by TSDC and DS can be compared with each other because the phenomena studied in both methods are determined by the dynamic behavior of the macromolecules. The relaxation processes displayed on both the $\epsilon^{\parallel} = \varphi(f)$ (DS) and $I = \varphi(T)$ (TSDC) plots are due to the orientation mobility of kinetic units containing a polar group. The temperature position of depolarization current peaks, T_m, formally corresponds to the temperature position of tgδ or ϵ'' peaks observed at the equivalent frequency f_e, which is in the range 10^{-2}−10^{-4} Hz.[4,5] Combination of DS and TSDS methods allows us to extend the interval of frequencies of measurements by TSDC and, in some cases, to resolve relaxation processes partly overlapping at higher frequencies.

In contrast to DS, the TSDC method is not isothermal, which is, in many respects, a disadvantage. However, using the thermal windowing technique, it is possible to determine the kinetic activation parameters of the observed relaxation processes at different temperatures.

In the present work a series of side-chain liquid-crystalline polymethacrylates PMm were investigated by TSDC and DS methods. Their general formula is as follows:

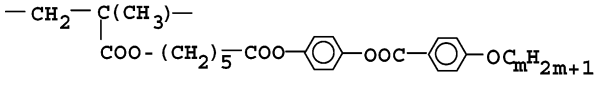

Here m ranges from 1 to 6. The phase transitions temperatures for PM1−PM6, glass transition temperature T_g determined by DSC, and T_m (temperature of the main global TSDC peak obtained from the $I = \varphi(T)$

* Corresponding author: e-mail nikon@imc.macro.ru; Fax (+007) 812-3286869; Tel (+007) 812-3288535.

10.1021/ma020832c CCC: $25.00
Published on Web 06/25/2003

Table 1. Temperature Transitions for PM1−PM6 Samples

sample	phase transitions (°C)	T_g[a] (°C)	T_m[b] (°C)
PM1	N 108 I	40	45
PM2	S_A 127 N 140 I	43	46
PM3	S_A 116 N 120 I	45	39
PM4	S_X 80 S_A 137 N 139 I	40	41
PM5	S_X 92 S_A 136 I	50	40
PM6	S_X 104 S_A 141 I	44	43

[a] Glass transition temperature obtained by DSC. [b] Temperature of depolarization current maximum on the global TSDC curve.

dependence) are presented in Table 1. The synthesis of these polymers has been described in ref 6.

The particular objectives of this work are as follows: (1) to study the molecular dynamics of the PM1−PM6 series by DS and TSDS methods, (2) to identify the observed processes of relaxation of dipole polarization, and (3) to determine the influence of terminal methylene mesogen sequence length on the kinetic characteristics of the relaxation transitions.

2. Experimental Part

Dielectric measurements were carried out by a Schlumberger FRA 1260 frequency response analyzer with a variable range buffer amplifier. A two-terminal plate capacitor (Novocontrol) was used in combination with an Ando type TO-19 thermostatic oven. The temperature dependence of tgδ was obtained with the aid of a conductivity and capacitance bridge of the TR-9701 type. The samples were sandwiched at 145 °C (in the isotropic state) between brass electrodes. The diameter of the potential electrode was 20 mm. The sample thickness of 50 μm was maintained by using 50 μm silica fibers.

TSDC experiments were carried out with a TSC-RMA (Thermhold) spectrometer on polymer pellets 0.34 mm thick and with a surface area of 76 mm^2. Two types of TSDC polarizing techniques were applied. (1) In the global experiments the sample was polarized by a dc electric field at a polarization temperature T_p, and it was then cooled to T_0 with the field still applied. The field was then removed, the sample was connected to an electrometer and heated at a constant rate r to a final temperature T_f, and the discharge current I was recorded as a function of temperature T. The experimental conditions were as follows: $T_p = 50$ °C for 2 min under a field of $U_p = 300$ V/mm, $T_0 = -160$ °C, $T_f = 70$ °C, and $r = 7$ °C/min. (2) In the thermal windowing experiments the polarizing field was applied only in a narrow temperature interval (window). The conditions in a series of thermal windowing experiments were as follows: poling windows 2 °C, temperature ranges from $T_p - 10$ °C to $T_p + 20$ °C, $r = 7$ °C/min, $U_p = 300$ V/mm.

3. Results and Discussion

3.1. Overall Behavior. For the PM1−PM6 series the dependence of dielectric permittivity ϵ' and of loss factor ϵ'' on frequency was obtained in the frequency range $10^{-2}-10^6$ Hz and in the temperatures range from room temperature to +160 °C. The temperature range included the glassy, the liquid-crystalline, and the isotropic states (Table 1). The shape of these dependences is similar for all PM1−PM6 samples and indicates that in the studied frequency and temperature intervals one or two overlapping relaxation processes exist. As an example, Figure 1 shows the $\epsilon'' = \varphi(f)$ plots for PM5 at several temperatures. One can see that for the first relaxation process observed in the LC smectic phase S_X (Table 1) the dielectric loss factor intensity, ϵ''_m, is about 0.01−0.1. At the transition from the smectic S_X to the smectic S_A phase, the dielectric losses increase sharply. In the S_A state two overlapping processes of dipole polarization are detected. For these processes the ϵ''_m

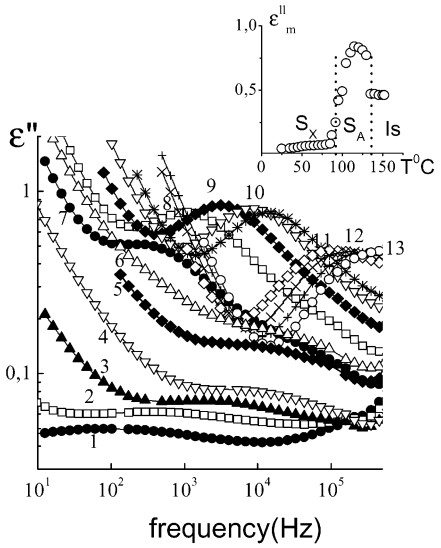

Figure 1. Frequency dependences of dielectric loss factor ϵ'' for PM5 at 30 (1), 50 (2), 70 (3), 85 (4), 87 (5), 92 (6), 95 (7), 105 (8), 115 (9), 125 (10), 135 (11), 145 (12), and 150 °C (13). The inset shows the temperature dependence of maximum loss factor ϵ''_m, where dashed lines correspond to the boundaries of the S_X and S_A phases and of the isotropic state.

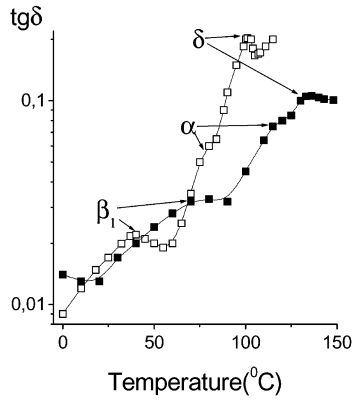

Figure 2. Temperature dependences of tgδ for PM6 at 0.1 kHz (□) and for PM1 at 100 kHz (■). The temperature positions of the β_1, α, and δ processes are shown by arrows.

values are 1 order of magnitude higher than those for the first process. In the isotropic state, at temperatures higher than the isotropic transition, T_{is}, one symmetric dielectric process is observed.

The temperature dependence of ϵ''_m shows a sharp change at 92 and 136 °C connected with the S_X/S_A and the T_{is} transitions, respectively (inset in Figure 1). Hence, the temperature dependence of the intensity of dielectric absorption can serve as an illustration of phase changes in polymers.

The temperature dependence of tgδ for PM1 and PM6 also indicates that in the investigated temperature range at least three relaxation processes occur (Figure 2). They will be further designated as the β_1, α, and, δ processes in the order of increasing temperature.

Besides dielectric study, the temperature dependences of depolarization current $I = \varphi(T)$ for the PM1−PM6 samples were obtained (Figure 3). This figure shows that two depolarization current peaks are observed for each sample. The first of them is located close to −10 °C, whereas the second, much more intensive global peak is observed at temperatures close to the glass transition temperature determined by DSC (Table 1).

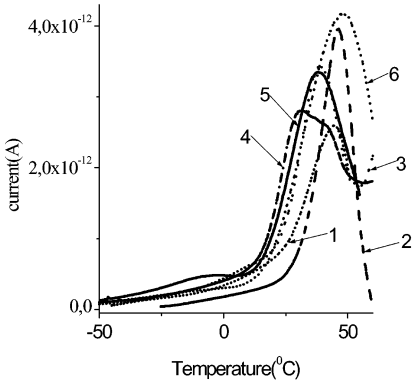

Figure 3. Global TSDC spectrum for PM1 (1), PM2 (2), PM3 (3), PM4 (4), PM5 (5), and PM6 (6).

Only in the case of PM4 the shape of the global peak shows clearly the overlapping of two processes.

To determine the kinetic characteristics of the observed relaxation processes, the frequency dependence of $\epsilon^{\parallel}$ was described by one or by a sum of two empirical Havriliak−Negami (HN) functions:[7,8]

$$[\epsilon^*(\omega) - \epsilon_\infty] = \Delta\epsilon[1 + (i\omega\tau_m)^{1-\alpha}]^{-\beta} \qquad (1)$$

where $\omega = 2\pi f$, τ_m is a relaxation time, $\tau_m = {}^1/_{2\pi f_m}$, where f_m is a characteristic relaxation rate, ϵ_∞ is the dielectric high-frequency permittivity, $\Delta\epsilon$ is the dielectric relaxation strength, representing the effective dipole moment of the reorienting unit, and α and β are fit parameters to describe the broadening and the asymmetry, respectively, of the relaxation time distribution. The contribution to $\epsilon^{\parallel}$ provided by the dc conductivity is also taken into account by the following term:[9]

$$\epsilon^{\parallel}_{\sigma} = \sigma/(\epsilon_0 2\pi f^S) \qquad (2)$$

where σ (the specific conductivity of the sample) and $S \leq 1$ are fit parameters, f is the frequency of the ac electric field, and ϵ_0 is the vacuum permittivity.

As an example of the analysis, Figure 4 shows the $\epsilon^{\parallel} = \varphi(f)$ dependence for PM5 at 95 °C given as a sum of contributions of the α and δ processes and of conductivity, which were calculated in accordance to eqs 1 and 2, respectively.

The temperature dependences of the relaxation time for the β_1, α, and δ processes obtained from the HN equation are presented in Figure 5 by curves 1, 2, and 3, respectively.

3.2. The β_1 Process. Figure 5 shows that in the range of the β_1 process the relaxation times for PM1−PM6 are practically identical. In the temperature range studied, the dependence of relaxation time on temperature can be described by the Arrhenius equation:

$$\tau_m(T) = \tau_0 \exp\left(\frac{E_a}{RT}\right) \qquad (3)$$

where the activation energy E_a is independent of temperature, τ_0 is a high-temperature limited relaxation time, and R is the gas constant 8.314 J/(K mol). E_a and τ_0 calculated according to eq 3 take values 18−20 kcal/mol and 10^{-16}−10^{-18} s, respectively, for the various PM1−PM6. Dielectric processes with relaxation times and activation energies almost coinciding with those observed in the present work have also been detected

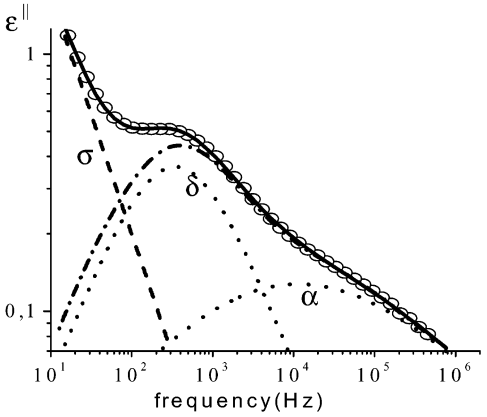

Figure 4. Frequency dependence of $\epsilon^{\parallel}$ for PM5 at 95 °C. The hollow circles are the experimental points. The solid line is the best fit given by the superposition of a conductivity term σ **(**dashed line**),** calculated according to eq 2, and of contributions due to the α and δ processes (dotted lines), calculated according to the HN function. The dashed−dotted line is the contribution due to dipole relaxation (fit curve without the conductivity term). The fitting parameters are as follows: $\sigma = 7 \times 10^{-10}$ 1/(Ω cm), $S = 0.93$; for the α process: $\Delta\epsilon = 0.82$, $\alpha = 0.41$, $\beta = 0.8$, $\tau_m = 7.9 \times 10^{-5}$ s; for the δ process: $\Delta\epsilon = 1.01$, $\alpha = 0.8$, $\beta = 1$, $\tau_m = 6.1 \times 10^{-4}$ s.

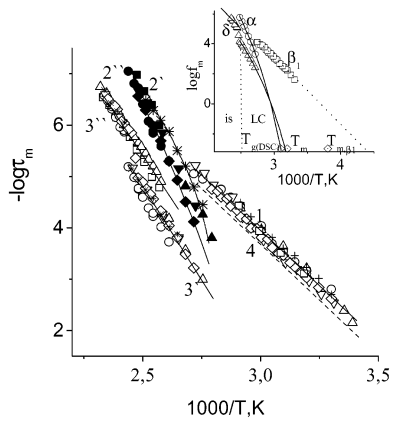

Figure 5. Dependence of −log τ_m on inverse temperature in the range of the β_1 (1), α (2), and δ (3) processes for PM1 (□, ■), PM2 (○, ●), PM3 (△, ▲), PM4 (▽, ▼), PM5 (◇, ♦), and PM6 (+, *); dashed line 4 corresponds to the β process in PMA-1, PMA-2, and PMA-3.[13] The inset shows the log $f_m = \varphi(1/T)$ dependence for PM5 in the range of the β_1, α, and δ processes.

in polymethacrylates with various structures, including side-chain LC polymethacrylates.[10−12]

To determine the molecular mechanism responsible for the β_1 process in the PM1−PM6 systems, the dielectric behavior in the series of polymethacrylates (PMA-*n*) and of polyacrylates (PA-*n*) will be considered. It is known that in PMA-*n* and PA-*n* the orientation of the single polar ester group adjoining the main chain is realized in two steps. As a result, two relaxation processes related to the mobility of ester groups, the local β process in the glassy state and the cooperative α relaxation, are revealed.[11,13−15] In the first numbers of PMA-*n* and PA-*n* series, the temperature of the α transition and, correspondingly, the T_g values decrease with increasing n due to internal plastification.[15] The same effect was observed for the local β process in PA-*n*. As for the β process, in the first numbers of PMA-*n*, for PMMA ($n = 1$), PEMA ($n = 2$), and PPMA ($n = 3$), the temperature dependences of relaxation times are

described by a single curve (Figure 5, curve 4[11,13]). This means that for the first normal homologues of PMA-*n* the relaxation times and their activation energies for the β process are almost independent of side chain length. At the same time one can see that the temperature−frequency coordinates of the β_1 process for PM1−PM6 (curve 1 in Figure 5) are very close to curve 4. This provides the basis for connecting the β_1 process in the PM1−PM6 series with the mobility of esters groups adjoining the main chain.

The experimentally observed coincidence of relaxation times in the first normal homologues of PMA-*n* and in the SCLCPs seems unexpected and requires additional discussion. It was shown that in the PMA-*n* series, at least in the first homologues, the steric factor predominates because the α-methyl groups in polymethacrylates provide spatial limitations to ester group rotation.[13] In PMA-*n* the ester group rotation, providing the contribution to the β process, becomes possible only near the α transition, since it requires local displacement of the bonds adjoining the main chain.

In the range of radio frequencies, beginning from PBMA ($n = 4$) and for PMA-*n* with *n* up to 8−9 (not yet crystallized), the α process (shifting to lower temperatures with increasing of side chain length) merges with the β process. For these systems, only one $\alpha\beta$ relaxation process takes place.[11,15] However, in PBMA it is possible to observe separately the α and β processes if the glass transition temperature and, consequently, the α transition temperature are increased. Thus, in ref 16 the β process was observed in PBMA for which the increase in T_g was achieved by using high hydrostatic pressure (higher than 1000 bar). In the same way, in random copolymers of butyl methacrylate with styrene it was also possible to observe the β process caused by ester group orientation.[17,18] This fact was explained by two effects. First, the β process moves to lower temperatures due to decreasing number of α-methyl groups. Second, the introduction of styrene into the macromolecule increases the T_g of the copolymer since the T_g of polystyrene is 50−60 °C higher than that of PBMA. In PBMA the α and β relaxation processes were also observed separately at low frequencies (10^{-2}−10^{0} Hz), whereas in the range of radio frequencies these two processes were extracted by analysis by means of the HN equation.[19]

In crystallized side-chain or side-chain LC polymers, the kinetic rigidity of the main chain increases owing to side-chain interactions. The segmental motion becomes hindered, and T_g increases. Accordingly, in such systems the α transition is displaced to higher temperatures, thus allowing us to observe the relaxation transition caused by the mobility of ester groups adjoining the main chain. The almost complete coincidence of relaxation times and activation energies of the β_1 process in PM1−PM6 and those of the β process in the first homologues of PMA-*n* results from the similarity of kinetic elements and from the orientation mechanism corresponding to the movement of ester groups adjoining the backbone.

Additional information on the β_1 process is obtained by the TSDC method. It is reasonable to assume that the first peak near −10 °C on the $I = \varphi(T)$ dependence in Figure 3 could be also related to the β_1 process. For comparing the DS and TSDC data in the range of the β_1 process, the $\log f_m = \varphi(1/T)$ dependence for this process was extrapolated to the equivalent frequency of 10^{-3} Hz. The linear extrapolation to 10^{-3} Hz (inset in Figure 5) gives a lower temperature value (−32 °C) than that actually obtained from the TSDC curve. This fact can be explained by the following considerations. For PM1−PM6 series, the E_a and $-\log \tau_0$ values in the range of the β_1 process in the Arrhenius equation are higher than those usually observed for local relaxation processes. For the latter processes, the E_a and τ_0 values are within the limits of 6−12 kcal/mol and 10^{-11}−10^{-13} s, respectively. The linear extrapolation of the $\log f_m = \varphi(1/T)$ dependences over a wide temperature and frequency ranges is actually valid only for local processes. In the case of PM1−PM6, linear extrapolation of the $\log f_m = \varphi(1/T)$ dependence (by more than 4 decades) for the β_1 process is probably not quite correct. It is possible to assume that in the case of the β_1 process the movement of ester groups in side-chain LC polymethacrylates exhibits some cooperativity, which results in a certain curvature of the $\log f_m = \varphi(1/T)$ dependence at low frequencies.

The fact that the β_1 process for the PM1−PM6 series is described by a single curve shows that, first, the molecular mobility of this process does not depend on the methylene sequence length on the mesogen tail. Second, the independence of the motion of the ester group adjoining the backbone from the other lateral chain part is provided by the flexible spacer consisting of five methylene groups.

3.3. The α and δ Processes. Near T_g, the dielectric dependences for SCLCPs show two cooperative processes, the α and δ processes.[3,12,20−24] The α process is related to segmental mobility and to contribution due to mesogen group reorientation about its long axis. The δ process, located at higher temperatures, reflects mesogen group reorientation about the short axis.

Taking into account the above considerations, the two overlapping relaxation processes near T_g observed for PM1−PM6 on the $\epsilon'' = \varphi(f)$ and $\mathrm{tg}\delta = \varphi(T)$ plots in Figures 1 and 2, respectively, can also be assigned to the α and δ processes. The coexistence of these processes in side-chain LC PM1−PM6 polymers indicates that mesogen groups and main chains, separated by a flexible methylene group spacer, move independently from each other. For PM1−PM6 the less intensive α process is shown as a shoulder on the well-determined δ peak (Figures 1 and 2). Hence, the parameters of the δ process are usually determined with a greater accuracy than those of the α process.

The relaxation times of the α and δ processes for the PM1−PM6 series are shown in Figure 5 by curves 2 and 3, respectively. It can be seen that the relaxation times for the PM1−PM6 series in the range of the α transition are rather close to each other and are in a "corridor" between curves 2′ and 2″, corresponding to PM6 and PM5, respectively. This is due to the fact that the difference between the T_g values of these polymers is small.

In the range of the δ process, the relaxation time values are grouped for the PM1−PM6 series near curves 3′ and 3″, corresponding to the liquid-crystalline and to the isotropic state, respectively. (Only for PM2 the relaxation times of the δ process in the LC state slightly deviate from curve 3′.)

For the α transition, in a wide temperature range, the $\log \tau_m = \varphi(1/T)$ dependence for SCLCPs, just as for polymers of other classes, cannot be described by the Arrhenius equation with one relaxation time. As usual,

the cooperative forms of molecular motion, in particular the α transition, are well described by the empirical Vogel−Tamman−Fulcher−Hesse (VTFH) equation:[25]

$$f_m = A \exp\left(-\frac{B}{T - T_0}\right) \quad (4)$$

where A, B, and T_0 are temperature-independent empirical parameters. A is a high-temperature limited relaxation rate, B is the activation parameter, and T_0, called the Vogel temperature or the ideal glass transition temperature, is usually by a few tens of degrees below T_g.

The temperature dependences of relaxation times for PM5 and PM6 in the range of the α process (Figure 5, curves 2″ and 2′) were fitted by the VTFH equation. The fit parameters for PM5 are $A = 10^{14}$ Hz, $B = 1397$ K, and $T_0 = 243$ K, whereas those for PM6 are $A = 10^{12}$ Hz, $B = 897$ K, and $T_0 = 256$ K. To determine the T_g from dielectric data, the VTFH dependence in the range of the α process should be extrapolated to the equivalent frequency $f_e = 10^{-3}$ Hz. For PM5 the extrapolated T_g value (inset in Figure 5) is 50 °C. This corresponds to the glass transition temperature, determined by DSC, and exceeds by 10 °C the peak temperature T_m on the global TSDC curve (Table 1). The T_g for PM6, obtained by extrapolation of curve 2′ to the equivalent frequency, is 42 °C. This value is close to T_g determined by DSC and to T_m obtained from the TSDC global curve (Table 1).

Unfortunately, it was not reliably possible to determine the temperature−frequency coordinates of the α process for all systems investigated here. However, it is evident that the mesogen tail length influences weakly the main chain mobility.

In the isotropic state, the temperature dependence of relaxation time in the range of the δ process for the PM1−PM6 series (Figure 5, curve 3″) can be described by the Arrhenius eq 3 with E_a equal to 34 kcal/mol.

The temperature dependence of relaxation time for the δ process occurring in the LC state can be described by the Arrhenius[20,26,27] or the VTFH equation.[28] In the case of PM5, the log $f_m = \varphi(1/T)$ dependence for the δ process taking place in the LC state was described by the VTFH equation with fit parameters $A = 10^{11}$ Hz, $B = 1207$ K, and $T_0 = 231$ K. The transition temperature of the δ process determined by extrapolation of the fit curve to the equivalent frequency 10^{-3} Hz is 44 °C (inset in Figure 5), i.e., lower than that for the α process.

In side-chain LC polymers, including PM1−PM6 studied here, the δ process observed on the temperature dependences of tgδ and of ϵ'' usually takes place in the viscous−elastic state at temperatures 5−20 °C higher than the α process.[3,20−24,26] This fact is not surprising since the reorientation of mesogens about the short axis requires a large free volume and takes place only in conditions of segmental mobility of the backbone. The inset in Figure 5 shows that the log $f_m = \varphi(1/T)$ dependences for the α and δ processes intersect near $\tau \sim 1$ s. It is apparent that the extrapolation of the log $f_m = \varphi(1/T)$ dependence in the range of the δ process to times lower than 1 s has no physical sense because this would mean that the δ process precedes the α process on the temperature scale and takes place in the glassy state. This fact requires more experimental data, and we plan to consider this phenomenon in the future.

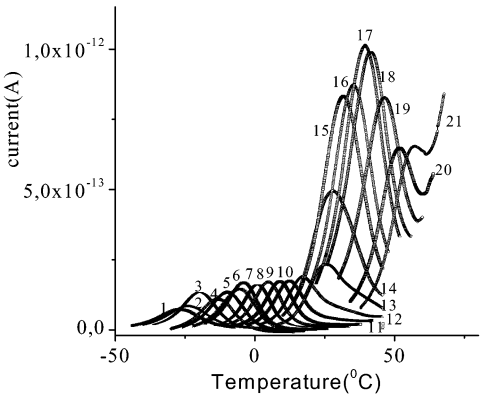

Figure 6. Set of elementary windowing curves for PM5 obtained at the poling temperatures: −35 (1), −31 (2), −27 (3), −23 (4), −17 (5), −13 (6), −9 (7), −5 (8), −1 (9), 3 (10), 7 (11), 11 (12), 15 (13), 19 (14), 23 (15), 27 (16), 31 (17), 35 (18), 39 (19), 43 (20), and 47 °C (21).

Figure 5 also shows that for the PM1−PM6 series the relaxation times in the range of the δ process are independent of mesogen tail length. This independence means that the δ process for the polymers studied here is eventually determined by the longitudinal component of the dipole moment of the mesogen, and the contribution to the dielectric spectrum coming from the reorientation of the ether group adjoining the mesogen is negligible.

It should be mentioned that for the PM1−PM6 series the discontinuity in the temperature dependence of relaxation time for the δ process (transition from curve 3′ to curve 3″ in Figure 5) takes place at temperatures close to the isotropization temperature, T_{is}. The jump in relaxation times at T_{is} transition for PM1−PM6 is 5−7 times. Similar results were obtained in refs 12, 20, 26, and 27. The increase in mesogen mobility at the transition from the mesophase to the isotropic state is a clear indication of the order disappearance and of the decrease in intermolecular interactions.[29]

3.4. Thermal Windowing TSDC Experiments. The thermal windowing TSDC experiments allow us to activate a narrow segment of the global spectrum on the temperature dependence of depolarization current. This gives us the opportunity to present a wide relaxation spectrum as a sequence of elementary components with one relaxation time and to calculate the kinetic characteristics of relaxation processes. In some cases, the thermal windowing experiments makes it possible also to separate overlapping processes.[29−35]

In the present work thermal windowing TSDC experiments were performed for the PM1−PM6 polymers. Figure 6 shows, as an example, the series of elementary components for PM5. One can see that at 16−20 °C there is a transition from a relaxation process of low intensity to the main global peak. According to the above considerations, the first relaxation area, at temperatures lower than 16−20 °C, could be attributed to the β_1 process. As for the main peak at high temperatures, one can observe at 45 °C the transition from the α to the δ process. (Unfortunately, because of the high conductivity level, the method of thermal windowing experiments was limited to polarization temperatures not exceeding 45−55 °C.)

In the calculation of the activation parameters it was assumed that each elementary component could be described by a curve with one relaxation time. The

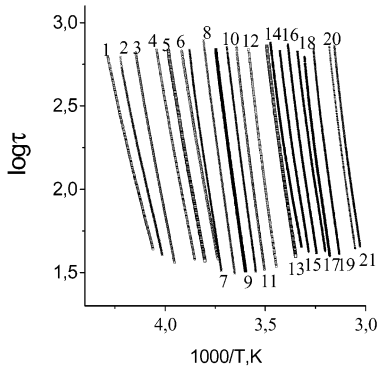

Figure 7. Arrhenius plots for PM5 obtained by integration of the elementary windowing curves in Figure 6.

temperature dependence of relaxation time could be described by the following expression[36]

$$\tau^{-1}(T) = \frac{rJ(T)}{\int_{T_0}^{T} J(T)\,\mathrm{d}T} \tag{5}$$

where r is the heating rate and T_0 is the low-temperature limit on the elementary curve. The integration of eq 5 allows us to pass from the temperature dependence of depolarization current to the temperature dependence of relaxation time for each elementary component.

Figure 7 shows the $\log \tau = \varphi(1/T)$ dependences for PM-5, where each elementary curve corresponds to its own polarization temperature T_p. It may be assumed that the temperature dependence of relaxation time obey to the Arrhenius (3) or to the Eyring (6) equation:

$$\tau(T) = \frac{h}{kT}\exp\left(\frac{\Delta G}{kT}\right) \tag{6}$$

where

$$\Delta G = \Delta H - T_m \Delta S \tag{7}$$

For PM1−PM6 the values of τ_0 and E_a, from eq 3, and ΔG (Gibbs energy), ΔH (enthalpy), and ΔS (entropy), from eq 6, were determined for each elementary component. Then, the dependences of E_a, τ_0, ΔG, ΔH, and ΔS on the maximum temperature T_m of the elementary peaks were plotted. These dependences are of common character for all PM1−PM6 systems. As an example, the dependences of τ_0, ΔG, ΔH, and ΔS on T_m are shown in Figure 8 for PM4 (E_a, repeating of ΔH is not shown). It is clear that these dependences are divided into three parts having two breaks at 30 and 45 °C. The similar dependences were obtained for some thermotropic side-chain polymers.[30,31] The portions of these dependences were related to the segmental mobility and to the α and δ relaxation.

The highest values of activation parameters are usually observed at T_m close to T_g. This is valid for PM1, PM2, and PM3 (inset in Figure 8) for which the highest values of ΔH were observed at 40−45 °C close to the T_g values observed by DSC (Table 1). (For PM3 the changes in ΔH, as well as in other activation parameters, at the break points are small.) At the same time, for the PM4−PM6 polymers with longer mesogen tails, the highest values of E_a, τ_0, ΔH, and ΔS were observed at temperatures 10−15 °C below T_g determined by DSC.

For many polymers, the results obtained by means of thermal windowing experiments show that, over a

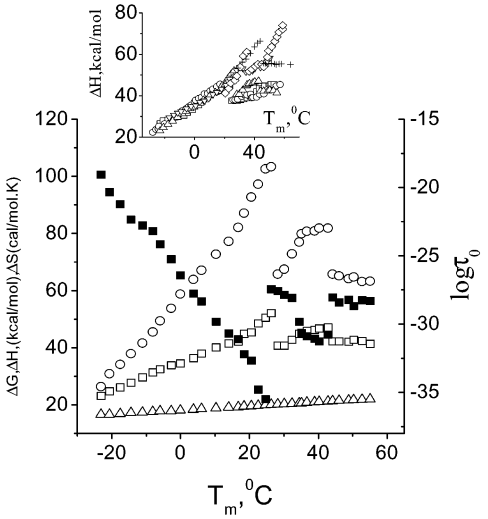

Figure 8. Gibbs free energy ΔG (△), enthalpy ΔH (□), entropy ΔS (○), and preexponential factor log τ_0 (■) on polarization temperature T_m for PM4. The inset shows the activation enthalpy ΔH vs T_m for PM1 (□), PM2 (○), PM3 (△), PM4 (▽), PM5 (◊), and PM6 (+).

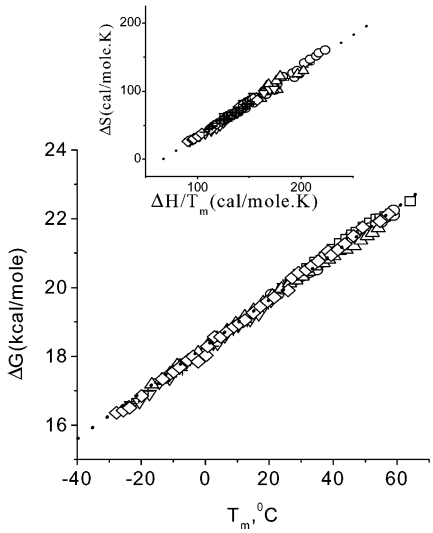

Figure 9. Gibbs free energy ΔG on T_m for PM1 (□), PM2 (○), PM3 (△), PM4 (▽), PM5 (◊), and PM6(+); the dashed line corresponds to the slope equal to 67 cal mol^{-1} K^{-1}. The inset shows the activation entropy ΔS vs $\Delta H/T_m$ PM1 (□), PM2 (○), PM3 (△), PM4 (▽), PM5 (◊), and PM6 (+); the dashed line corresponds to the slope equal to 1.

wide temperature range covering both local and cooperative processes, there is a linear dependence between ΔG and the temperature of maximum on the elementary curve,[30,31] i.e.

$$\Delta G = aT_m \tag{8}$$

where a is 67 cal K^{-1} mol^{-1}. The dependences $\Delta G = aT_m$ are given for PM1−PM6 in Figure 9. It is seen that these dependences lie on a straight line corresponding to a slope of 67 cal K^{-1} mol^{-1} (dashed line in Figure 9). It follows from eqs 7 and 8 that

$$\Delta S = (\Delta H/T_m) - a \tag{9}$$

Equation 9 means that there is a linear dependence between ΔS and $\Delta H/T_m$. As expected, the $\Delta S = \varphi(\Delta H/T_m)$ dependences for PM1−PM6 are on a dashed line

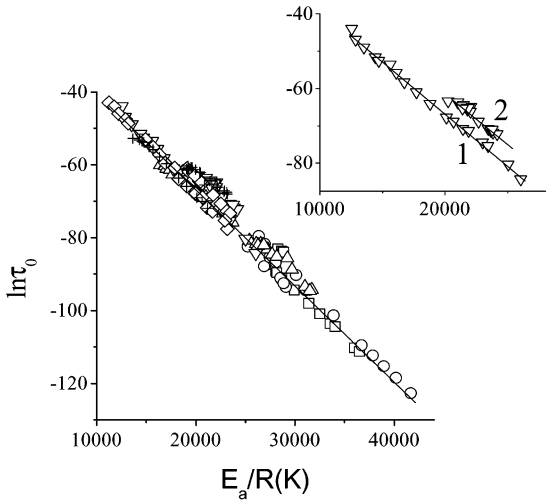

Figure 10. Logarithm of the preexponential factor ln τ_0 on activation energy E_a/R for PM1 (□), PM2 (○), PM3 (△), PM4 (▽), PM5 (◇), and PM6 (+). The inset shows the same dependence for PM4 in the ranges of the α(1) and δ(2) processes.

with slope equal to 1 and interception point equal to $-a$ (inset in Figure 9). The data in Figure 9 show that the free Gibbs energy depends only on temperature and does not depend on the structure, and the ΔS and ΔH values are interrelated. This means that the $\Delta S = \varphi(\Delta H/T_m)$ and the $\Delta G = \varphi(T_m)$ dependences can be considered to be calibration curves, since it is sufficient to know one parameter in order to determine the other one.

3.5. Compensation Law. It was shown that for thermal windowing experiments a series of elementary curves in the glass transition temperature range obey the so-called compensation law.[30−34] This law is valid when the activation parameters increase with temperature. The compensation law is characterized by two phenomenological parameters: compensation temperature T_c and compensation relaxation time τ_c.

Within the framework of the Arrhenius model, the compensation law is expressed by a linear dependence of the preexponential factor on the activation energy.[32−37]

$$\tau_0 = \tau_c \exp(-E_a/RT_c) \qquad (10)$$

It follows from eq 10 that the slope and the intersection of the $\ln(\tau_0) = \varphi(E_a/R)$ dependence determine the values of $(-1/T_c)$ and ln τ_c, respectively. Figure 10 presents the $\ln(\tau_0) = \varphi(E_a/R)$ dependences for PM1−PM6. It is shown that these dependences lie down virtually on one straight line. This means that the compensation parameters for the PM1−PM6 series are close to each other. The compensation parameters determined from the $\ln(\tau_0) = \varphi(E_a/R)$ dependence for PM4 (curve 1, inset in Figure 10) are $T_c = 335$ K ($-1/T_c = -0.00298$) and $\tau_c = 9.5 \times 10^{-4}$ s (ln $\tau_c = -6.7$). The glass transition temperature determined by DSC is equal to 40 °C (313 K) for PM4; i.e., it is by 22 °C lower than T_c. For various polymers, the differences between the compensation temperature and the glass transition temperature, $\Delta T = T_c - T_g$, are usually 5−30 K.[32−35,38] The compensation parameter values for the Arrhenius and the Eyring models are generally close to each other, and they differ within the experimental error.

Figure 10 shows also that, in addition to the straight line 1 describing the compensation behavior of the PM1−PM6 polymers, there is a group of points that do not fall on this straight line. For all these polymers, the straight line 2 can be plotted. As an example, this line is shown for PM4 in the inset in Figure 10. Curve 2 on the $\ln(\tau_0) = \varphi(E_a/R)$ dependences is observed only for thermotropic side-chain polymers[33] and could be related to the δ process, which occurs only in SCLCPs and is absent in polymers of other classes. It is necessary to note that calculation of activation parameters from thermal windowing experiments has formal character.

Until now, there is no common understanding of the physical sense of the compensation behavior in polymers. There are some approaches making it possible to relate this phenomenon to the chemical structure of polymers[33] and to the thermal expansion coefficient[39] or to explain the compensation behavior by means of the coupling model.[40] Despite great differences in the approaches (including the opinion that the compensation parameters have no physical sense[32]), they are widely used for describing the results of investigation of polymers by the TSDC method.

4. Conclusions

A number of side-chain LC polymethacrylates with various lengths of the tail mesogen group were investigated by DS and TSDC methods. In the temperature range from room temperature to 160 °C, three processes of relaxation of dipole polarization, the β_1, α, and δ processes, were revealed. Molecular mechanisms of the β_1, α, and δ processes are related to the mobility of ester groups adjoining the backbone, to the segmental motion, and to the mesogen group orientation about its short axis, respectively. It was shown that the molecular mobility of the observed relaxation processes does not depend on the mesogen tail length. This means that the kinetic units responsible for the appearance of the β_1, α, and δ processes do not include the methylene sequence on the mesogen end. The comparison of the DS and TSDC data with each other gives good agreement between the temperature position of dielectric loss peaks at the equivalent frequency of TSDC measurements and the temperature position of depolarization current maximum. By using thermal windowing techniques, the activation parameters for the observed processes were determined.

Acknowledgment. The authors gratefully acknowledge the financial support of the University of Valencia and of the Greek Ministry of National Economy, Directorate for International Economic Organizations (academic year 2001).

References and Notes

(1) Moscicki, J. K. In *Liquid Crystal Polymers: From Structure to Applications;* Collyer, A. A., Ed.; Elsevier: London, 1992; Chapter 4, pp 143−236.
(2) Simon, G. P. In *Dielectric Spectroscopy of Polymeric Materials;* Runt, J. P., Fitzgerald, J. J., Eds.; American Chemical Society: Washington, DC, 1997; Chapter 12, pp 329−378.
(3) Zentel, R.; Strobl, G. R.; Ringsdorf, H. *Macromolecules* **1985**, *18*, 960−965.
(4) Van Turnhout, J. In *Thermally Stimulated Discharge of Polymer Electrets*; Elsevier Scientific: Amsterdam, 1975.
(5) Boersma, A.; Van Turnhout, J.; Wubbenhorst, M. *Macromolecules* **1998**, *31*, 1**,** 7453−7460.
(6) Tao Yongjie. Synthesis, Structure and Conformation of Macromolecules of Comb-Like Liquid-Crystalline Polymethacrylates. Ph.D. Thesis, Moscow State University, Moscow, 1999.

(7) Havriliak, S.; Negami, S. *J. Polym. Sci., Polym. Symp.* **1966**, *14*, 89.
(8) Havriliak, S.; Negami, S. In *Dielectric and Mechanical Relaxation in Materials*; Hanser: Munich, 1997.
(9) Bottcher, C. J. F.; Bordewijk, P. In *Theory of Electcric Polarization*, 2nd ed.; Elsevier: Amsterdam, 1978; Vol. 2, p 72.
(10) Sanchis, M. J.; Diaz-Calleja, R.; Gargallo, L.; Hormazabal, A.; Radic, D. *Macromolecules* **1999**, *32*, 3457−3463.
(11) McCrum, N. G.; Read, B. E.; Williams, G. In *Anelastic and Dielectric Effects in Polymeric Solids*; Wiley: New York, 1967.
(12) Nikonorova, N. A.; Borisova, T. I.; Barmatov, E. B.; Pissis, P.; Diaz-Calleja, R. *Polymer* **2002**, *43*, 2229−2238.
(13) Mikhailov, G. P.; Borisova, T. I. *Zh. Techn. Phys.* **1958**, *28*, 137−142.
(14) Beiner, M.; Schroter, K.; Hempel, E.; Reissing, S.; Donth, E. *Macromolecules* **1999**, *32*, 6278−6282.
(15) Borisova, T. I.; Burshtein, L. L.; Shevelev, V. A.; Shibaev, V. P.; Plate, N. A. *Vysokomol. Soedin., Ser. A* **1973**, *15*, 674−679.
(16) Williams, G.; Edwards, D. A. *Trans. Faraday Soc.* **1966**, *62*, 1329−1335.
(17) Mikhailov, G. P.; Borisova, T. I.; Nigmankhodzhaev, A. S. *Vysokomol. Soedin., Ser. A* **1966,** *8*, 969−975.
(18) Mikhailov, G. P.; Borisova, T. I.; Ivanov, N. N.; Nigmankhodzhaev, A. S. *Vysokomol. Soedin., Ser. A* **1967**, *9*, 778−784.
(19) Garwe, F.; Schonhals, A.; Lockwenz, H.; Beiner, M.; Schroter, K.; Donth, E. *Macromolecules* **1996**, *29*, 247−253.
(20) Nikonorova, N. A.; Borisova, T. I.; Shibaev, V. P. *Macromol. Chem. Phys.* **2000**, *201*, 226−232.
(21) Valerien, S. U.; Kremer, F.; Boeffel, C. *Liq. Cryst.* **1990**, *4*, 79−86.
(22) Araki, K. *Polym. J.* **1990**, *22*, 546−550.
(23) Pramoto, H.; Bormuth, F. G.; Haase, W. *Makromol. Chem.* **1987**, *187*, 2453−2459.
(24) Mijovic, J.; Sy, J.-W. *Macromolecules* **2000**, *33*, 9620−9629.
(25) Ngai, K. L.; Schonhals, A.; Schlosser, E. *Macromolecules* **1992**, *25*, 4915−4921.
(26) Kresse, H.; Kostromin, S. G.; Shibaev, V. P. *Makromol. Chem., Rapid Commun.* **1981**, *3*, 509−513.
(27) Simon, R.; Coles, H. J. *J. Polym. Sci., Part B: Polym. Phys.* **1989**, *27*, 1823−1836.
(28) Zhong, Z. Z.; Schule, D. E.; Smith, S. W.; Gordon, W. L. *Macromolecules* **1993**, *26*, 6403−6409.
(29) Seiberle, H.; Stille, W.; Strobl, G. *Macromolecules* **1990**, *23*, 2008−2016.
(30) Mura-Ramos, J. J.; Mano, J. F.; Lacey, D.; Nestor, G. *J. Polym. Sci., Part B: Polym. Phys.* **1996**, *34*, 2067−2075.
(31) Mano, J. F.; Correia, N.; Moura-Ramos, J. J.; Andrews, S. R.; Williams, G. *Liq. Cryst.* **1996**, *20*, 201−217.
(32) Sauer, B. B.; Mura-Ramos, J. J. *Polymer* **1997**, *38*, 4065−4069.
(33) Mura-Ramos, J. J.; Mano, J. F.; Sauer, B. B. *Polymer* **1997**, *38*, 1081−1089.
(34) Teyssedre, G.; Lacabanne, C. *Phys. D: Appl. Phys.* **1995**, *28*, 1478−1487.
(35) Doulut, S.; Bacharan, C.; Demont, P.; Bernes, A.; Lacabanne, C. *J. Non-Cryst. Solids* **1998**, *235−237*, 645−651.
(36) Bucci, C.; Fieschi, R. *Phys. Rev. Lett.* **1964**, *12*, 16−19.
(37) Mano, J. F.; Mura-Ramos, J. J.; Fernandes, A.; Williams, G. *Polymer* **1994**, *35*, 5170−5178.
(38) Lacabanne, C.; Lamure, A.; Teyssedre, G.; Bernes, A.; Mourgues, M. *J. Non-Cryst. Solids* **1994**, *172−174*, 884−890.
(39) Sauer, B. B.; Avakian, P. *Polymer* **1992**, *31*, 5128−5136.
(40) Ngai, K. L.; Rendell, R. W.; Ragajopal, A. K.; Teiler, S. *Ann. N.Y. Acad. Sci.* **1986**, *484*, 150−156.

MA020832C